

**Analysis of the effect of oxygen doping and pressure
on superconducting transition temperature in metal oxides**

A. A. Kosov

Mari State University, Yoshkar-Ola,

Mari El, 424001 Russia

E-mail: kosov@margu.mari.ru

R. I. Boughton

Bowling Green State University, Bowling Green,

Ohio, 43402 USA

E-mail: boughton@bgnet.bgsu.edu

Submitted: January , 1998

Abstract

The two-orbital Hubbard model is used to obtain formulas for the fermion excitation spectrum in the energy bands hybridized by the Anderson interaction. An analysis of the lower part of the energy spectrum leads to a formula for the superconducting transition temperature T_c associated with the pairing of quasiparticles in one of the correlated bands. The dependence of T_c upon pressure is analyzed, and the individual influence of carrier density enhancement and interaction strength is obtained as a function of oxygen concentration. The experimental discrimination made by Honma et al ^a in $Y_{0.9}Ca_{0.1}Ba_2Cu_3O_{7-\delta}$ by separating out the contributions due to carrier density and pairing strength can be reproduced quantitatively, and perhaps with

further refinement, so can the carrier concentration. Although the prediction of the absolute value of the transition temperature is not accurate using the present model, it is clear that it furnishes a reasonably accurate description of the change in transition temperature with pressure. The component contributions due to change in carrier concentration and due to change in interaction strength as a function of oxygen concentration are also in reasonable agreement with the experimental results.

a. T. Honma, K. Yamaya, N. Mori, and M. Tanimoto, *Solid State Commun.* **98**, No.5, 395-399 (1996).

I. INTRODUCTION

The investigation of the mechanism of superconductivity in cuprate superconductors is related to the effects of oxygen doping and pressure on the superconducting transition temperature (T_c) of these substances. One of the advantages of using high pressure techniques is the ability to change atomic distances without substitution of components, which often causes some side effects^{1,2}. At the present time several review articles concerning high-pressure work in cuprate superconductors have been published. According to the experimental results and the conclusions of Shafer et al.³ and Kubo et al.⁴, the carrier concentration increases with increasing pressure in many high- T_c materials. This increase in carriers is considered to be due to charge transfer from a charge reservoir layer to the Cu-O plane. The evidence for the dependence of the carrier concentration upon pressure comes from measurements of the Hall

number $1/eR_H$ and the thermoelectric power under high-pressure. Generally, T_c initially increases with increasing $1/eR_H$, but decreases when $1/eR_H$ exceeds a specific value. However, the relation between T_c and $1/eR_H$ in high-pressure experiments varies among different cuprate superconductors. For instance, in La-Sr-Cu-O ceramics, T_c increases with increasing pressure, but no change in $1/eR_H$ is observed. On the other hand, in the case of Y-Ba-Cu-O, a variation of T_c with $1/eR_H$ is observed by several authors in high-pressure experiments. It was proposed⁵ that the change in T_c due to pressure (ΔT_c) should be expressed as the sum of two terms, $(\Delta T_c)_c$ and $(\Delta T_c)_p$, where $(\Delta T_c)_c$ is the change in T_c due to pressure-induced changes in the carrier density, and $(\Delta T_c)_p$ is the change in T_c due to pressure-enhanced electron pairing (e.g., change in the electron-phonon coupling strength, or in the exchange coupling constant). Honma et al.⁶ investigated the dependence of T_c on the Hall number by changing the oxygen content and the pressure in $Y_{0.9}Ca_{0.1}Ba_2Cu_3O_y$. They determined that the contribution of $(\Delta T_c)_c$ to (ΔT_c) increases with decreasing oxygen content.

In this work we use the idea that $(\Delta T_c) = (\Delta T_c)_c + (\Delta T_c)_p$ and apply the Anderson-Hubbard two orbital model⁷ to describe the experimental results of Ref. 6. In Section II we introduce the Hamiltonian of the problem, the Green's functions of the quasiparticles in correlated bands, and the equation for T_c . Section III is devoted to the calculation of the pressure effect on the superconducting transition temperature. By proposing a simple relation between the value of pressure P and the width of the correlated band W , the dependence of T_c on pressure can be

obtained. In addition, a comparison with experimental results on the dependence of T_c , (ΔT_c) , $(\Delta T_c)_c$ and $(\Delta T_c)_p$ on the concentration of carriers in YCaBaCuO is made. Good agreement between the theoretical calculation of the dependence of (ΔT_c) , and $(\Delta T_c)_c$ on pressure, and the experimental results is found. It is concluded that the model under consideration is quite promising for studying the effects of oxygen doping and pressure on the superconducting transition in cuprate superconductors.

II. FORMULATION

One of the popular models used for describing a strongly correlated system is the Hubbard model. Recently Kosov and Shilov^{7,8} studied the superconducting transition and pressure effects by using a unified Hamiltonian containing operators of the Hubbard two-orbital model and the Anderson interaction. The interaction considerably enhances the applicability of the Hubbard model and allowed the authors to describe the interaction of non-localized and localized electrons by proceeding from the mixing of their one-particle states.

The model in Refs.7,8 is based on the following Hamiltonian:

$$H = H_0 + H_{\text{int}} = \sum H_{0i} + \sum t_{ij} C_{is}^+ C_{is} \quad (1)$$

$$H_{0i} = -\mu (n_{ia\uparrow} + n_{ia\downarrow} + n_{ic\uparrow} + n_{ic\downarrow}) + E (n_{ia\uparrow} + n_{ia\downarrow}) -$$

$$\begin{aligned}
& - H (n_{ia\uparrow} - n_{ia\downarrow} + n_{ic\uparrow} - n_{ic\downarrow}) + I n_{ia\uparrow} n_{ia\downarrow} + U(n_{ia\uparrow} + n_{ia\downarrow}) (n_{ic\uparrow} + \\
& \quad n_{ic\downarrow}) + U_1 n_{ic\uparrow} n_{ic\downarrow} + \\
& \quad + V_0 (a_{i\uparrow}^{\dagger} C_{i\uparrow} + a_{i\downarrow}^{\dagger} C_{i\downarrow} + \text{h.c.}),
\end{aligned}$$

where C_{is}^{\dagger} , C_{is} and a_{is}^{\dagger} , a_{is} are field operators corresponding to free and localized electrons at the site i with spin projection s ; $n_{ias} = a_{is}^{\dagger} a_{is}$ and $n_{ics} = C_{is}^{\dagger} C_{is}$ are the operators for the number of electrons; \mathbf{S}_i and \mathbf{s}_i are the spin operators of c - and a - electrons; μ is the chemical potential; H is the applied magnetic field; E the one-particle energy of the a - electrons; I , U , and U_1 are the energy parameters defining intra-atomic correlation; I is the Hubbard interaction between localized electrons; U is the inter-orbital Coulomb interaction of c - and a - electrons; U_1 is the repulsive interaction of c -electrons on one site; V_0 is the matrix element responsible for the hybridization of the c - and a - electronic states (Anderson's constant); and H_{int} describes the interstitial tunneling of c -electrons with transport integral t_{ij} .

Diagonalization of the single-cell Hamiltonian H_{0i} and a transition to Hubbard's operators X_p^q leads to the following results for the wave function and the energy spectrum:

$$E_0 = 0, \quad \Psi_0 = |0, 0\rangle - \text{vacuum state};$$

$$E_{A,B} = -\mu + (E - 2H)/2 \pm ((E/2)^2 + (V_0)^2)^{1/2};$$

$$\Psi_{A,B} = \cos(\alpha) |+, 0\rangle \pm \sin(\alpha) |0, +\rangle;$$

$$E_{C,D} = -\mu + (E + 2H)/2 \pm ((E/2)^2 + (V_0)^2)^{1/2};$$

$$\Psi_{C,D} = \cos(\alpha) |-, 0\rangle \pm \sin(\alpha) |0, -\rangle;$$

$$|s, 0\rangle = a_{is}^+ |0, 0\rangle; \quad |0, +\rangle = C_{is}^+ |0, 0\rangle.$$

$$\cos(\alpha) = Z/(Z^2 + V_0^2)^{1/2}; \quad \sin(\alpha) = V_0/(Z^2 + V_0^2)^{1/2}$$

$$Z = \begin{cases} ((E/2)^2 + (V_0)^2)^{1/2} + E/2, & \text{if } E > 0; \\ ((E/2)^2 + (V_0)^2)^{1/2} - E/2, & \text{if } E < 0; \end{cases}$$

It was mentioned in the Introduction that the one-particle states A, B, C, and D depend on the energy V_0 . We find:

$$E_{F,G} = U - 2\mu + E \pm 2H;$$

$$\Psi_F = |+, +\rangle; \quad \Psi_G = |-, -\rangle;$$

$$E_T = U - 2\mu + E;$$

$$\Psi_S = 2^{-1/2} \{ |+, -\rangle - |-, +\rangle \};$$

$$|+, +\rangle = a_{i\uparrow}^+ C_{i\uparrow}^+ |0, 0\rangle; \quad |-, -\rangle = a_{i\downarrow}^+ C_{i\downarrow}^+ |0, 0\rangle;$$

$$|+, -\rangle = a_{i\uparrow}^+ C_{i\downarrow}^+ |0, 0\rangle.$$

The energy of the remaining two-particle states E_K , E_L , and E_M can be obtained by using the cubic equation:

$$X^3 + A X^2 + B X + C = 0; \quad (2)$$

$$A = - (I + U + U_1 + 3E); \quad B = (I + 2E)(I + U) + U_1 (3E + U + I) - 4(V_0)^2;$$

$$C = 2(V_0)^2 (I + 2E + U_1) - U_1(E + U)(2E + I).$$

The roots $X = \{X_m\}$ of Eq. (2) define the energy $E_{K,L,M}$: $X_m = 2\mu + E_m$, $m = K, L, M$. It must be emphasized that a consideration of two-particle states is the most significant aspect of this research, and distinguishes it from the widely discussed calculation of T_c in the t-J model⁹, which does not directly take into consideration the two-particle electron states at a single site.

After exact diagonalization of the single-lattice part of the Hamiltonian (1), it can be represented in terms of Hubbard diagonal operators X_p^q in the following form⁹:

$$H_{0i} = \sum E_P X_P^P; \quad (3)$$

$$P = 0, A, B, \dots, K, L, M.$$

The operator H_{int} responsible for interstitial electron jumps can be represented in a quadratic form using nondiagonal Hubbard operators:

$$H_{\text{int}} = \sum t_{ij} g_{is}^*(X) g_{js}(X). \quad (4)$$

a. $E > 0$;

$$C_{i\uparrow}^+ = \cos(\alpha)X_B^0 + R_D^K X_K^D = g_{i\uparrow}^*(X);$$

$$C_{i\downarrow}^+ = \cos(\alpha)X_D^0 + R_B^K X_K^B = g_{i\downarrow}^*(X);$$

$$R_D^K = R_B^K = \cos(\alpha)*(A_1B_2 - A_2B_1) + \sin(\alpha)*(A_1B_3 - A_3B_1)/\sqrt{2}.$$

b. $E < 0$;

$$C_{i\uparrow}^+ = \cos(\alpha)X_A^0 + R_C^K X_K^{DC} = g_{i\uparrow}^*(X);$$

$$C_{i\downarrow}^+ = \cos(\alpha)X_C^0 + R_A^K X_K^{BA} = g_{i\downarrow}^*(X);$$

$$R_C^K = R_A^K = \cos(\alpha)*(C_1A_3 - A_1C_3)/\sqrt{2} + \sin(\alpha)*(C_1A_2 - C_2A_1).$$

$$A_1 = (1 + A_{21}^2 + A_{31}^2)^{-1/2}; \quad A_2 = A_{21}*A_1; \quad A_3 = A_{31}*A_1;$$

$$A_{21} = (E_L - 2E - I)^2/2V_0^2; \quad A_{31} = (E_L - 2E - I)^2/(E_L - U_1)^2;$$

$$B_2 = (1 + B_{12}^2 + B_{32}^2)^{-1/2}; \quad B_1 = B_{12}*B_2; \quad B_3 = B_{32}*B_2;$$

$$B_{12} = [(E_M + 2E - U)(E_M - U_1) - 2V_0^2] / [\sqrt{2}V_0 (E_M - U_1)]; \quad B_{32} = \sqrt{2}V_0 / (E_M - U_1);$$

$$C_3 = (1 + C_{13}^2 + C_{23}^2)^{-1/2}; \quad C_1 = C_{13}C_3; \quad C_2 = C_{23}C_3;$$

$$C_{13} = [(E_K - E - U)(E_K - U_1) - 2V_0^2] / [2V_0^2]; \quad C_{23} = (E_K - U_1) / \sqrt{2}V_0;$$

$$E_K < E_M < E_L.$$

We assume that the density of states in the dispersion region has a rectangular shape:^{7,8,10}

$$\rho(\varepsilon) = (1/2W) \theta(W^2 - \varepsilon^2);$$

where $2W$ is the width of the c -band.

Carrying out calculations similar to those in Refs.7,10, we obtain the following expression for the chemical potential:

$$\mu = -\Delta/2 - WB_+/2 + 2(n_K + n_S) W (R_K^S)^2 - P./2; \quad (8)$$

$$P_{\pm} = \{B_+^2 W^2 \pm 2 \Delta_1 B.W + \Delta_1^2\}^{1/2};$$

$$B_{\pm} = \cos^2 \alpha (n_0 + n_Q) \pm (R_D^K)^2 (n_K + n_S).$$

The chemical potential μ is determined by the concentration of electrons in the dispersed correlated band, which equals $n_c = (R_K^S)^2 (n_K + n_S)$. The dependence of n_c and μ upon V_0 shows different behaviors in the cases $E > 0$ and $E < 0$. An increase in the hybridization parameter V_0 leads to a decrease in n_c when $E > 0$, and to an increase when $E < 0$.

A transition to the Hubbard operators allows the use of the Green's temperature function technique to take the interstitial jump term into account in order to study the superconducting properties of the model. An analysis of the lower part of the energy spectrum leads to the following formula for the superconducting transition temperature associated with the pairing of quasiparticles in one of the correlated bands:

$$T_c/2W = 0.57 [-\xi_{10}(-W) \xi_{10}(W)/W^2]^{1/2} \exp[-1/A(n, t_0)]; \quad (11)$$

$$\xi_{10}(-W) = -2 (R_K^S)^2 (n_K + n_S);$$

$$\xi_{10}(W) = -\mu + (B_+ W - P_+ - \Delta)/2;$$

$$A(n, t_0) = \Gamma(n, t_0)/\Lambda(n, t_0);$$

$$\Gamma(n, t_0) = t_0 \{ \cos^2(\alpha) (n_0 + n_Q) (E_S - E_K) (E_S + B_- t_0) +$$

$$+ (R_K^S)^2 (n_K + n_S) E_Q (E_Q - E_K + B_- t_0) \};$$

$$\Lambda(n, t_0) = W[B_+(2\mu + \Delta) + B_-\Delta](2\mu + \Delta - B_+t_0).$$

The quantity $A(n, t_0)$ plays the role of the quasiparticle scattering amplitude with different spin orientation. The attraction between quasiparticles in a correlated band takes place under the conditions:

$$A(n, t_0) > 0; \quad -W < t_0 < W; \quad \xi_{10}(W) \geq 0. \quad (12)$$

The conditions (12) can be used to determine the concentration $n_{S1} < n < n_{S2}$ for which $T_c \neq 0$. Solving the equation $\xi_{10}(W) = 0$ gives the following value for n_{S2} :

$$n_{S2} = 2\cos^2(\alpha)/[\cos^2(\alpha) + (R_K^S)^2]. \quad (12a)$$

The condition $A(n, t_0) = 0$ gives the following result for n_{S1} :

$$n_{S1} = 2\cos^2(\alpha)/[\cos^2(\alpha) + 2(R_K^S)^2]. \quad (12b)$$

In particular, if we put $V_0 = 0$ and $E > 0$ in (12a) and (12b), we obtain $n_{S1} = 2/3$ and $n_{S2} = 1$. This result has been obtained by Zaitsev and Ivanov¹¹ in the frame of the one-orbital Hubbard model (the so-called “kinematic mechanism of superconductivity”).

III. PRESSURE EFFECTS

In applying the two-orbital Anderson-Hubbard model to describe the pressure dependence of T_c , we choose to examine the energy parameters, which more sensitively depend on the value of pressure. Since U , I , U_1 , V_0 , and E are on-site properties, their pressure dependence can be neglected. The transport integral t_p depends on the spatial distribution of atoms and is changed by applied pressure. Let us consider the region where W depends linearly on t_p ($W \sim t_p$). According to Marsiglio and Hirsh¹², the transport integral in cuprate superconductors can be expressed through the lattice parameters of the CuO_2 planes a , b , and c by the formulas:

$$t_{||} = \hbar^2/(2m_{||}a); \quad t_{\perp} = \hbar^2/(2m_{\perp}c);$$

where $m_{||}$ and m_{\perp} are the respective effective masses.

Neglecting any pressure dependence of the effective masses, we estimate the magnitude of dW/dP :

$$dW/dP \sim dt_p/dP \sim -2W(d\ln a/dP) = 2Wk_a. \quad (13)$$

Here k_a , k_b , and k_c are the compressibility components along each crystallographic direction as defined by:

$$k_a = -d\ln a/dP; \quad k_b = -d\ln b/dP; \quad k_c = -d\ln c/dP.$$

In order to simplify the numerical estimation of the results, we consider the case $k_a = k_b = k_c$. Using the relations in the equation (13), the following expression for the dependence of the bandwidth upon pressure is obtained:

$$W(P) = W(P=0)\exp(2k_a P). \quad (14)$$

Formulas (11) and (14) allow us to express T_c as a function of pressure. Using expression (13) it is possible to obtain formulas for dT_c/dP and $d\ln T_c/dP$:

$$dT_c/dP = T_c d\ln T_c/dP \sim 2Wk_a (dT_c/dW); \quad (15)$$

$$dT_c/dW = (T_c/2W)\{1 + 2W[B_- + (B_+^2(P_+ - P_-)W - \Delta_1 B_- (P_+ + P_-)) / 2P_+ P_-] + (2W/A^2(n, t_0))(dA(n, t_0)/dW)\};$$

$$dA(n, t_0)/dW = -A(n, t_0)/W + \Lambda(n, t_0)^{-1} \{(2(2\mu + \Delta) - B_+ t_0)[\cos^2 \alpha(n_0 + n_Q)(E_S - E_K)(E_S + 2B_- t_0) + (R_K^S)^2 (n_K + n_S)E_Q(E_Q - E_K + 2B_- t_0) + A(n, t_0)B_+ W(B_+(2\mu + \Delta) + \Delta_1 B_-)] - 2WA(n, t_0)[2B_+(2\mu + \Delta) + \Delta_1 B_- - B_+^2 t_0]\}(d\mu/dW);$$

$$d\mu/dW = 2(R_K^S)^2 (n_K + n_S) - B_+/2 - (WB_+^2 - \Delta_1 B_-) / 2P_-.$$

By means of formula (15) we obtain a theoretical expression for $(\Delta T_c)_p$:

$$(\Delta T_c)_p = (dT_c/dP) * \Delta P = (dT_c/dW) * \Delta W. \quad (16)$$

To compare our results with the experimental data of Ref.6 we obtain the value $(\Delta T_c)_c$ from formula (11):

$$(\Delta T_c)_c = (dT_c/dn)^* \Delta n = (dT_c/dn)^* (dn/dP)^* \Delta P = (dT_c/dn)^* (dn/dW)^* \Delta W. \quad (17)$$

IV. DISCUSSION

We have chosen to compare the theoretical results presented in the previous section with the recent experimental results of Honma et al⁶, who studied the pressure dependence and the effect of oxygen doping on the transition temperature of the $Y_{0.9}Ca_{0.1}Ba_2Cu_3O_y$ (YCBCO) system. These authors systematically investigated the critical temperature dependence and the dependence of the Hall number $1/eR_H$, upon pressure, in order to be able to distinguish between those effects which result from changes in carrier density $(\Delta T_c)_c$, and changes in the coupling strength (electron pairing) $(\Delta T_c)_p$.

The first comparison we shall examine is the dependence of the critical temperature T_c , on the oxygen content y . The theoretical results for a pressure of 2 GPa and a compressibility k_a of 0.0024 GPa⁻¹ are displayed in Fig. 1, where 5 curves are plotted, each with a variation in one or more of the following bandwidth-normalized parameters: the single-particle energy $-E/W$, the inter-atomic correlation energies I/W , U_1/W , and U/W ; and the hybridization energy V_o/W . The values of the parameters used in the various curves used to fit the data are listed in Table I below:

TABLE I **Parameter Values Used**

Curve Number	$-E/W$	I/W	U_1/W	U/W	V_o/W
1	-1.9	6.0	3.5	2.4	1.8
2	-1.9	6.0	3.5	2.4	2.0
3	-1.7	6.0	3.5	2.4	1.8
4	-1.8	5.0	2.5	2.8	1.8
5	-1.9	6.0	2.4	3.5	2.0

The data of Fig. 1 in the paper by Honma et al. are represented by open circles. As can be seen from the figure, the general concave-down form of the experimental results can be qualitatively reproduced by the theoretical curves with the same maximum value, and with little variation exhibited for different parameter combinations. The requisite width of the curve exhibited by the experimental data is however not readily attained with any reasonable variation in the parameters. The difficulty in fitting the theory to an absolute quantity like the critical temperature is not unexpected, since the absolute values of the potentials chosen are involved in making such a comparison.

In Figs. 2a and 2b are plotted the critical temperature change at a pressure of 2 GPa and a compressibility k_a of 0.0024 GPa^{-1} , due to changes in carrier density and pairing strength $(\Delta T_c)_c$ and $(\Delta T_c)_p$, respectively, as a function of oxygen content y . Here, the agreement with the experimental results of Honma et al (open circles) is fairly good. Once again, the theoretical curves exhibit a concave down behavior over the range of y that was measured. Of the parameter sets chosen for illustration, it appears that the parameters corresponding to curve number 5 ($-E/W = -1.9$, $I/W = 6.0$, $U_1/W = 2.4$, $U/W = 3.5$, and $V_o/W = 2.0$) give the closest fit to the experimental data in both cases. Fig. 3 illustrates the sum of the two effects to give the total change in temperature, $(\Delta T_c)_c + (\Delta T_c)_p = \Delta T_c$ plotted vs. oxygen content y , along with the experimental data. Once again the theoretical treatment yields a set of concave down curves which qualitatively approximate the data with the best fit to the experimental data given by curve number 5. Over all, the theoretical model appears to quite accurately account for the observed experimental variation with oxygen content. In contrast with the first plot, these comparisons involve the change in critical temperature with pressure and so can be more realistically accounted for by the theoretical model.

For the Hall number $1/eR_H$, which should scale with the ratio of the carrier density enhancement of the critical temperature $(\Delta T_c)_c$ to the sum of the absolute values of the individual critical temperature

enhancements $\left(\frac{(\Delta T_c)_c}{|(\Delta T_c)_c| + |(\Delta T_c)_p|}\right)$, the plot vs. oxygen concentration y shown in Fig. 4 illustrates the comparison between theory and experimental data of Honma et al., who labelled this ratio α . Here the fit is not good with any of the parameter variations that were tried. Although the experimental data fall on curve 4 near $\Delta T_c / \left(\frac{(\Delta T_c)_c}{|(\Delta T_c)_c| + |(\Delta T_c)_p|}\right) = 1$, where the temperature change is almost entirely due to change in carrier concentration, the slopes are clearly not in agreement. We believe this discrepancy arises from the reduced accuracy in evaluating this fraction when the Hall coefficient changes sign, which it does in the case where $(y, \alpha) = (6.87, 0.39)$. The theoretical curve nevertheless gives a reasonable qualitative description of the variation in this parameter, as a decreasing function of oxygen content. In order to determine how $\frac{dT_c}{dn}$ varies with oxygen concentration y , we have used a third-order polynomial fit of the form: $dn(y) = a_3 y^3 + a_2 y^2 + a_1 y + a_0$. The fitting parameters are obtained by using the data of Honma et al. at $y = 6.59, 6.72$ and 6.87 , respectively, and by setting $dn(7.0) = 0$. The values of the fitting parameters are: $a_0 = -461.1850$; $a_1 = 141.5920$; $a_2 = -11.6100$; $a_3 = 0.1135$. This relation provides a reasonable idea about the strength of the effect of charge carrier density upon ΔT_c .

Finally, in Fig. 5, we plot the total change in the transition temperature vs. pressure as obtained from the theoretical model. The experimental results are shown as data points according to the legend. It is apparent that the quality of agreement is good, with no more than 10% discrepancy. The rate of increase in T_c with pressure is faithfully reproduced for all three fractional oxygen contents studied by Honma et al. It is important to note the nearly zero slope at the highest concentration, $y = 6.87$.

CONCLUSIONS

In this paper we have demonstrated that the application of the Hubbard model provides a good basis for describing the observed variation of the pressure dependence of the critical temperature on oxygen concentration in the $Y_{0.9}Ca_{0.1}Ba_2Cu_3O_y$ (YCBCO) system. It appears that the experimental discrimination made by Honma et al in separating out the contributions due to carrier density and pairing strength can be reproduced quantitatively, and perhaps with further refinement, so can the carrier concentration. Although the prediction of the absolute value of the transition temperature is not accurate using the present model, it is clear that it furnishes a reasonably accurate description of the change in transition temperature with pressure. The component contributions due to change in carrier concentration and due to change in interaction strength as a function of oxygen concentration are also in reasonable agreement with the experimental results.

REFERENCES

- ¹ J.S.Schilling and S.Klotz, Physical Properties of High Temperature Superconductors, Vol. III. ed. by D.M.Ginsberg, World Scientific, Singapore, 1992.
- ² H.Takahashi and N.Mori, Studies of High Temperature Superconductors, Vol.16. ed. by Anant Narlikar, Nova Science Publishers, INC, 1996.
- ³ M.W. Shafer, T. Penny, B.L. Olson, R.L. Greene, and R.H. Koch, Phys. Rev. **B39**, 2914 (1988).
- ⁴ Y. Kubo, Y. Shimakawa, T. Monako, and H. Igarashi, Phys. Rev. **B43**, 7875 (1991).
- ⁵ Y. Iye, J. Phys. Chem. Solid. **53**, 1561 (1992).
- ⁶ T. Honma, K. Yamaya, N. Mori, and M. Tanimoto, Solid State Commun. **98**, No.5, 395-399 (1996).
- ⁷ A.A.Kosov, and V.E.Shilov, Fiz. Nizk. Temp. **22**, 1032 (1996) [Low Temp. Phys. **22**(9), 787 (1996)].
- ⁸ A. A. Kosov, Fiz. Nizk. Temp. **24**, No. 3 (1998) [Low Temp. Phys. **24**(3), (1998)].
- ⁹ Yu.A.Izyumov, M.I.Katsnel'son, and Yu.N.Skryabin, *Magnetism of Collectivized Electrons*
[in Russian], Nauka, Moscow (1994).
- ¹⁰ P.B.Zyubin, V.A.Ivanov, and E.A.Ugol'kova, Teor.and Matem.Fiz. **101**, 304 (1994).
- ¹¹ R.O.Zaitsev, and V.A.Ivanov, Fiz.Tverd.Tela (Leningrad) **29**, 2554 (1987) [Sov.Phys. Solid State **29**, 1475 (1987)].
- ¹² Marsiglio, and J.E.Hirsh, Phys. Rev. **B41**, 6435 (1990).

CAPTIONS

FIG.1. Dependence of the function T_c on the oxygen content y for $Y_{0.9}Ca_{0.1}Ba_2Cu_3O_y$ obtained for the parameters $k_a=0.00024 \text{ GPa}^{-1}$; $P=2 \text{ GPa}$.

FIG.2a. Dependence of $(\Delta T_c)_p$ on the oxygen content y for $Y_{0.9}Ca_{0.1}Ba_2Cu_3O_y$ obtained for the parameters $k_a=0.00024 \text{ GPa}^{-1}$; $P=2 \text{ GPa}$.

FIG.2b. Dependence of $(\Delta T_c)_c$ on the oxygen content y for $Y_{0.9}Ca_{0.1}Ba_2Cu_3O_y$ obtained for the parameters $k_a=0.00024 \text{ GPa}^{-1}$; $P=2 \text{ GPa}$.

FIG.3. Dependence of $(\Delta T_c)_p + (\Delta T_c)_c$ on the oxygen content y for $Y_{0.9}Ca_{0.1}Ba_2Cu_3O_y$ obtained for the parameters $k_a=0.00024 \text{ GPa}^{-1}$; $P=2 \text{ GPa}$.

FIG.4. Dependence of the ratio $\alpha = |(\Delta T_c)_c| / (|(\Delta T_c)_p| + |(\Delta T_c)_c|)$ on the oxygen content y for $Y_{0.9}Ca_{0.1}Ba_2Cu_3O_y$ obtained for the parameters $k_a=0.00024 \text{ GPa}^{-1}$; $P=2 \text{ GPa}$.

FIG.5. T_c as a function of pressure in $Y_{0.9}Ca_{0.1}Ba_2Cu_3O_y$ (cross - $y = 6.59$, star - $y = 6.72$, open circle - $y = 6.87$ - experimental data⁶) obtained for the parameter $k_a=0.00024 \text{ GPa}^{-1}$ (used for curve 5).

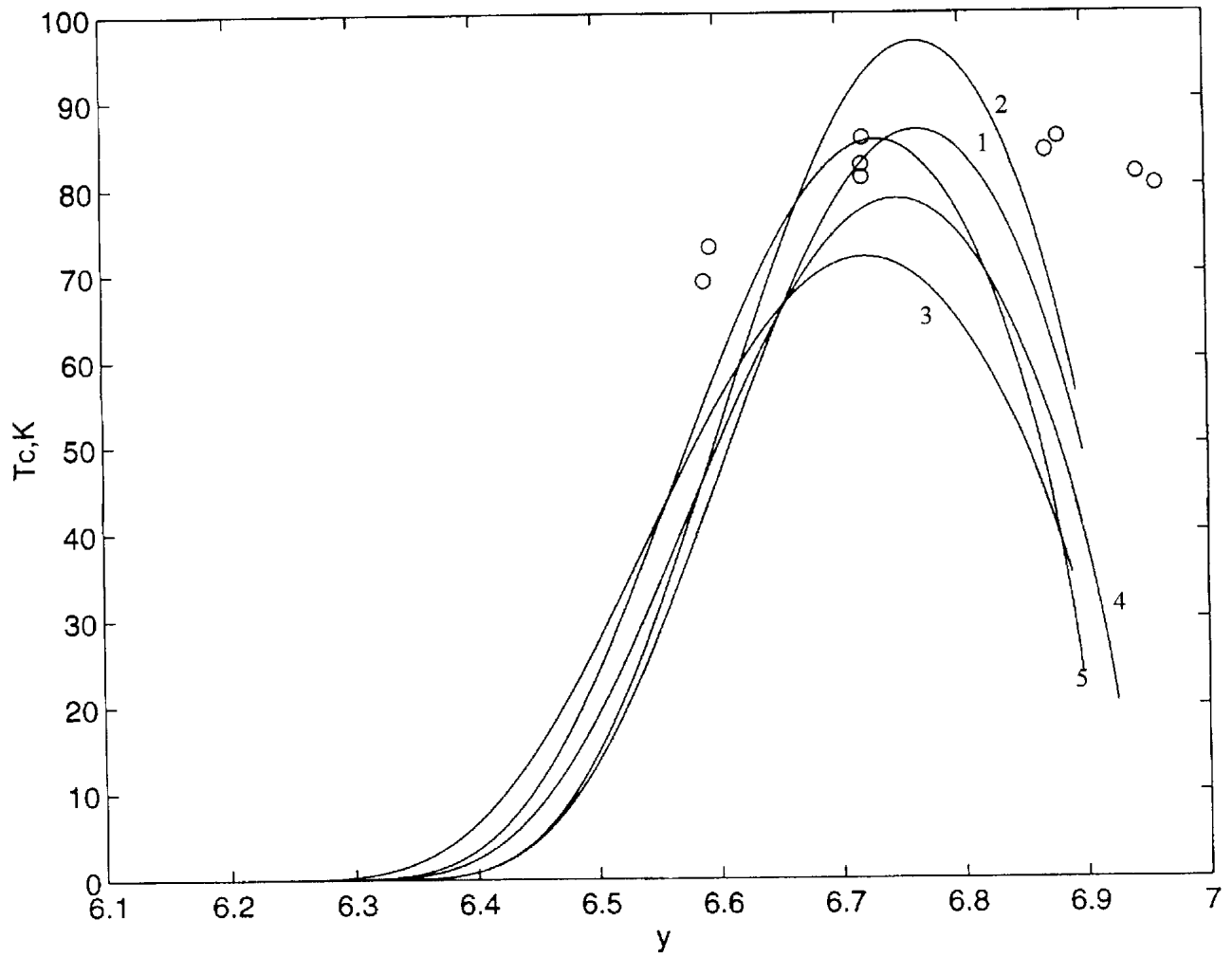


Figure 1

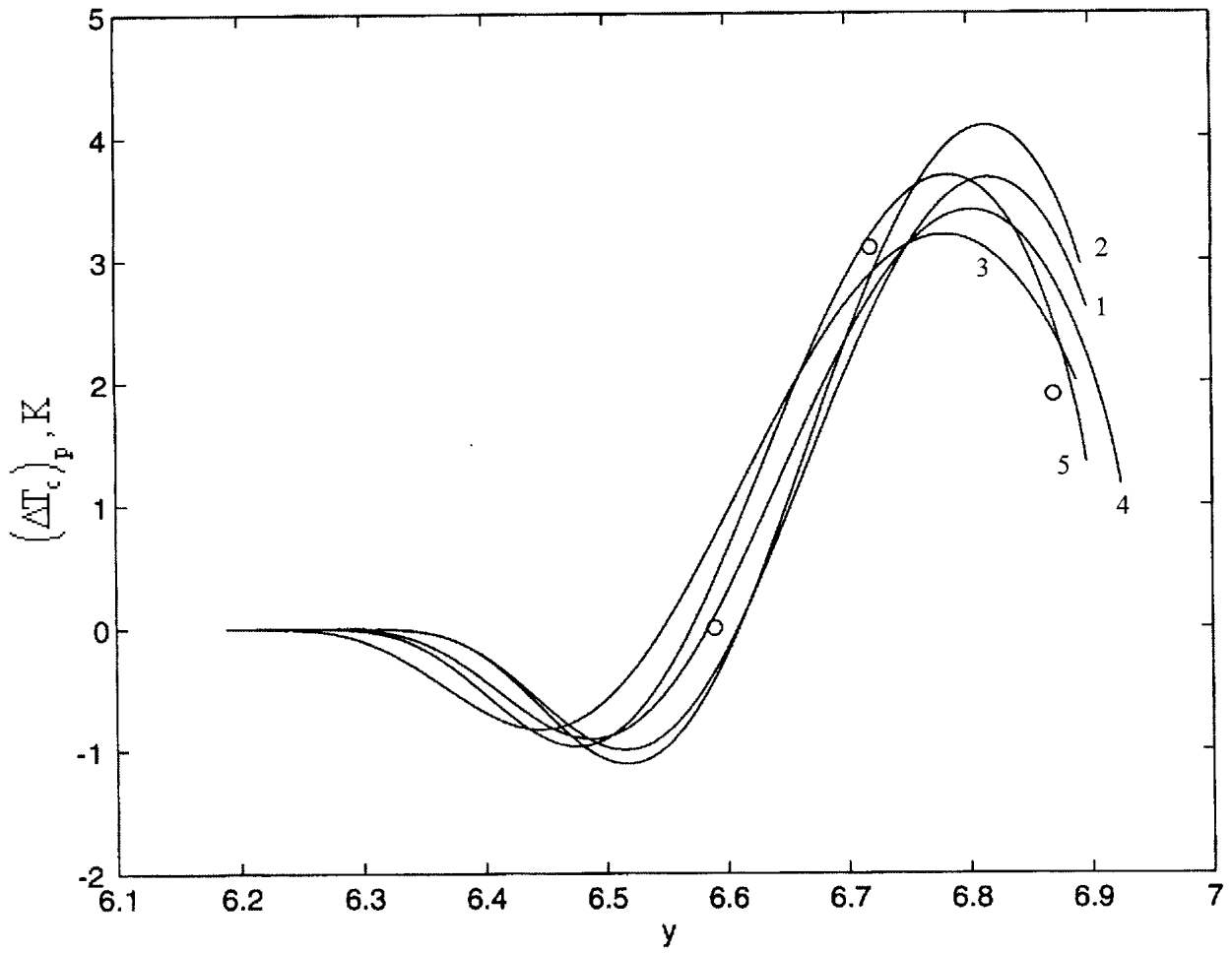


Figure 2

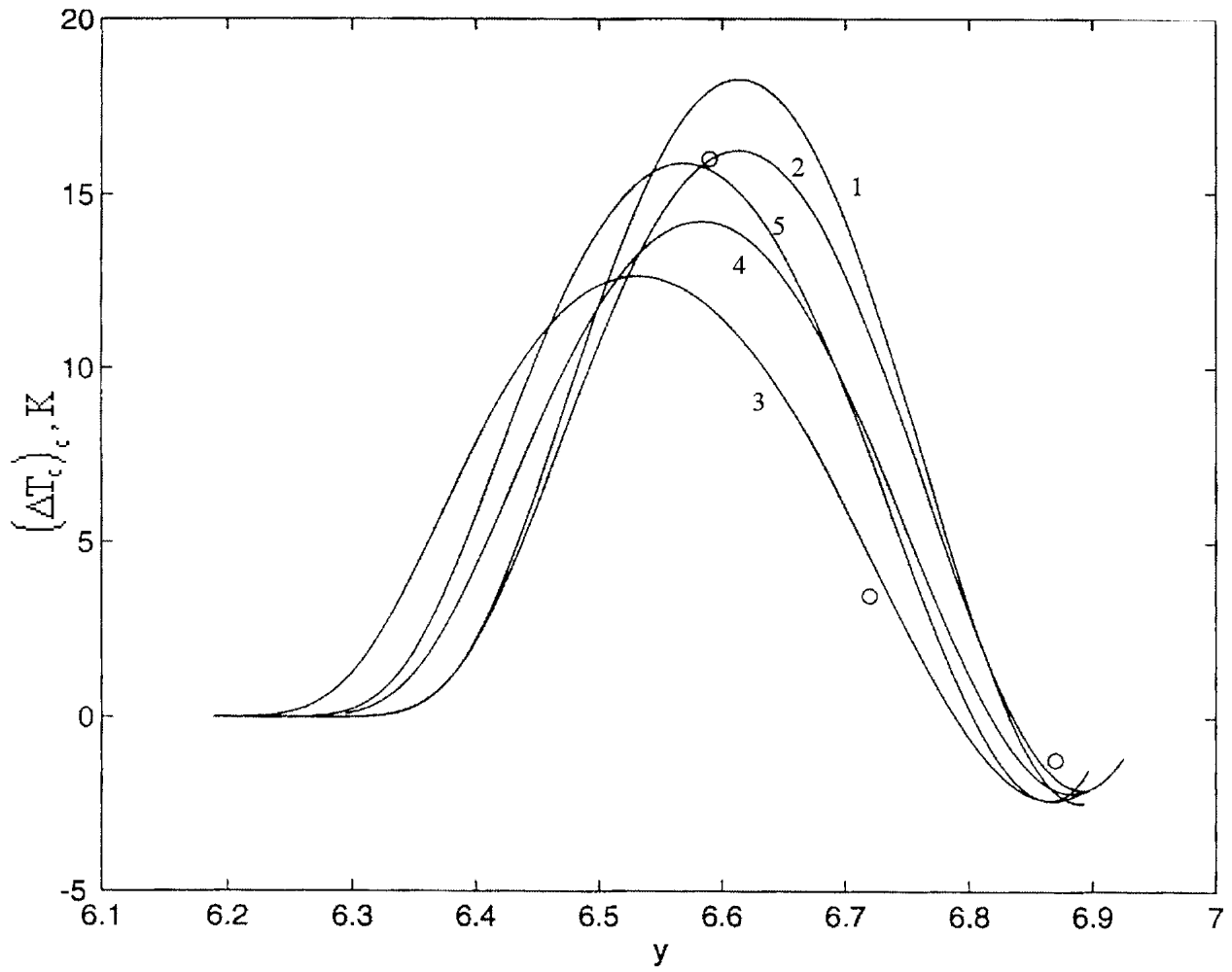


Figure 3

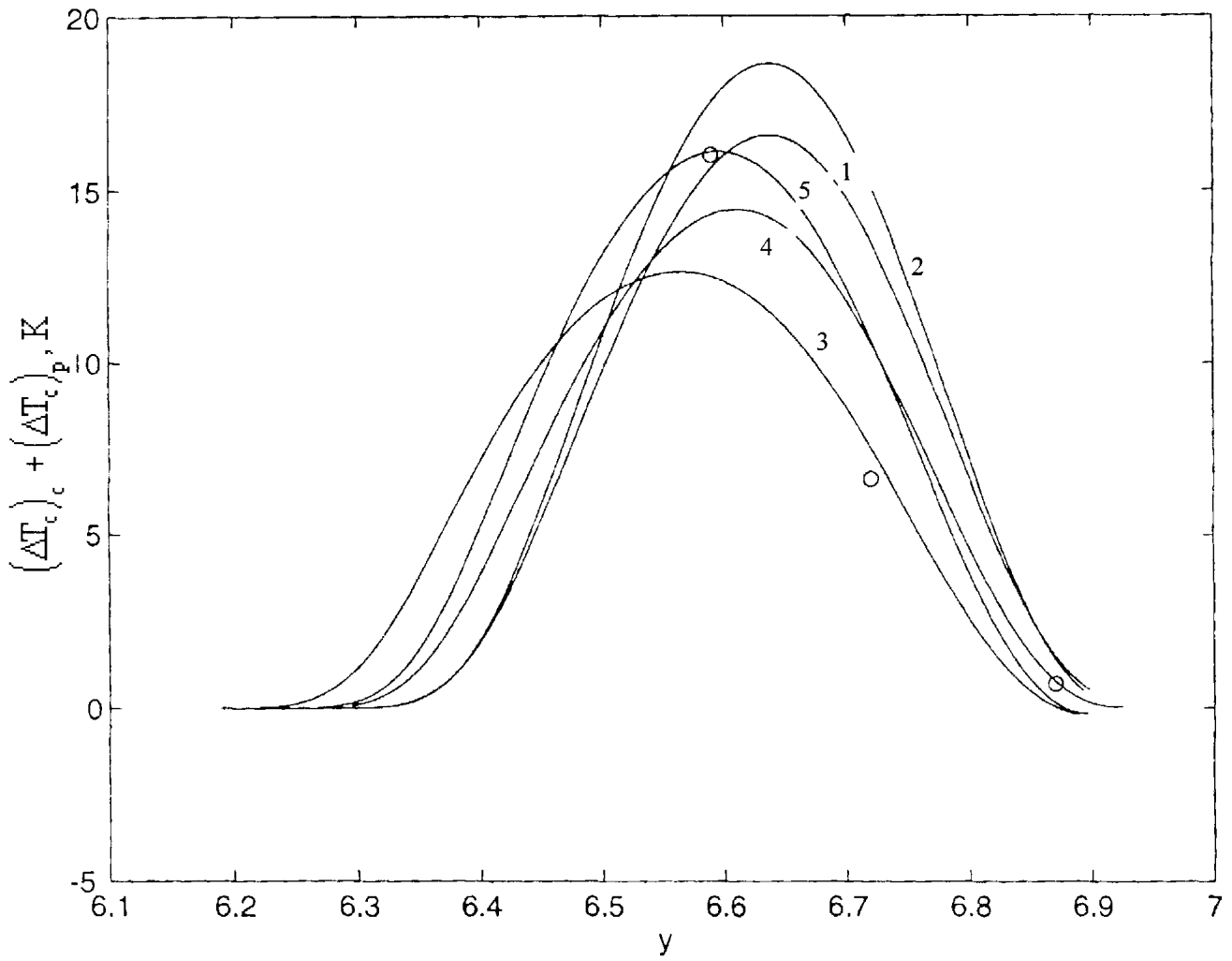


Figure 4

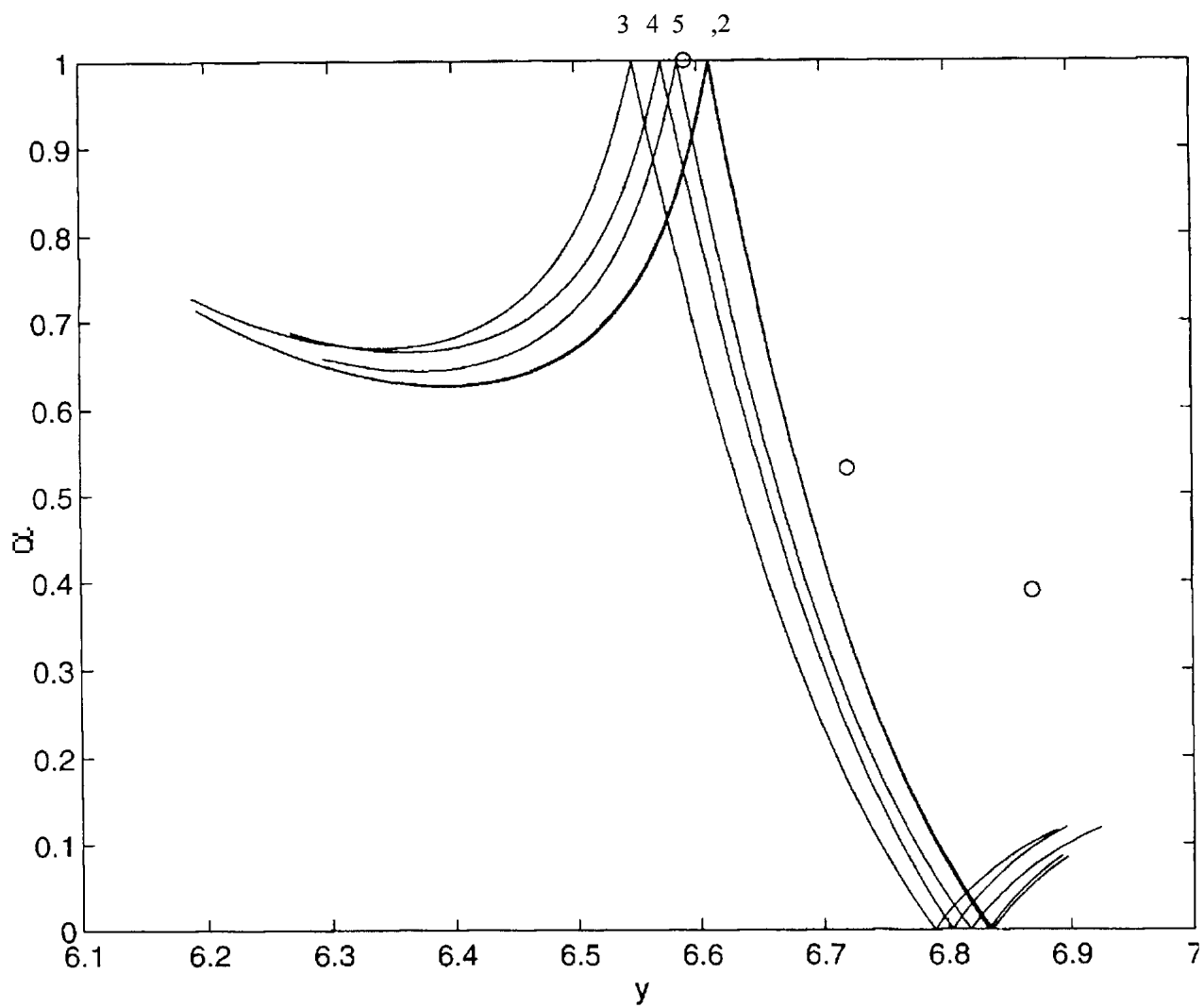


Figure 5

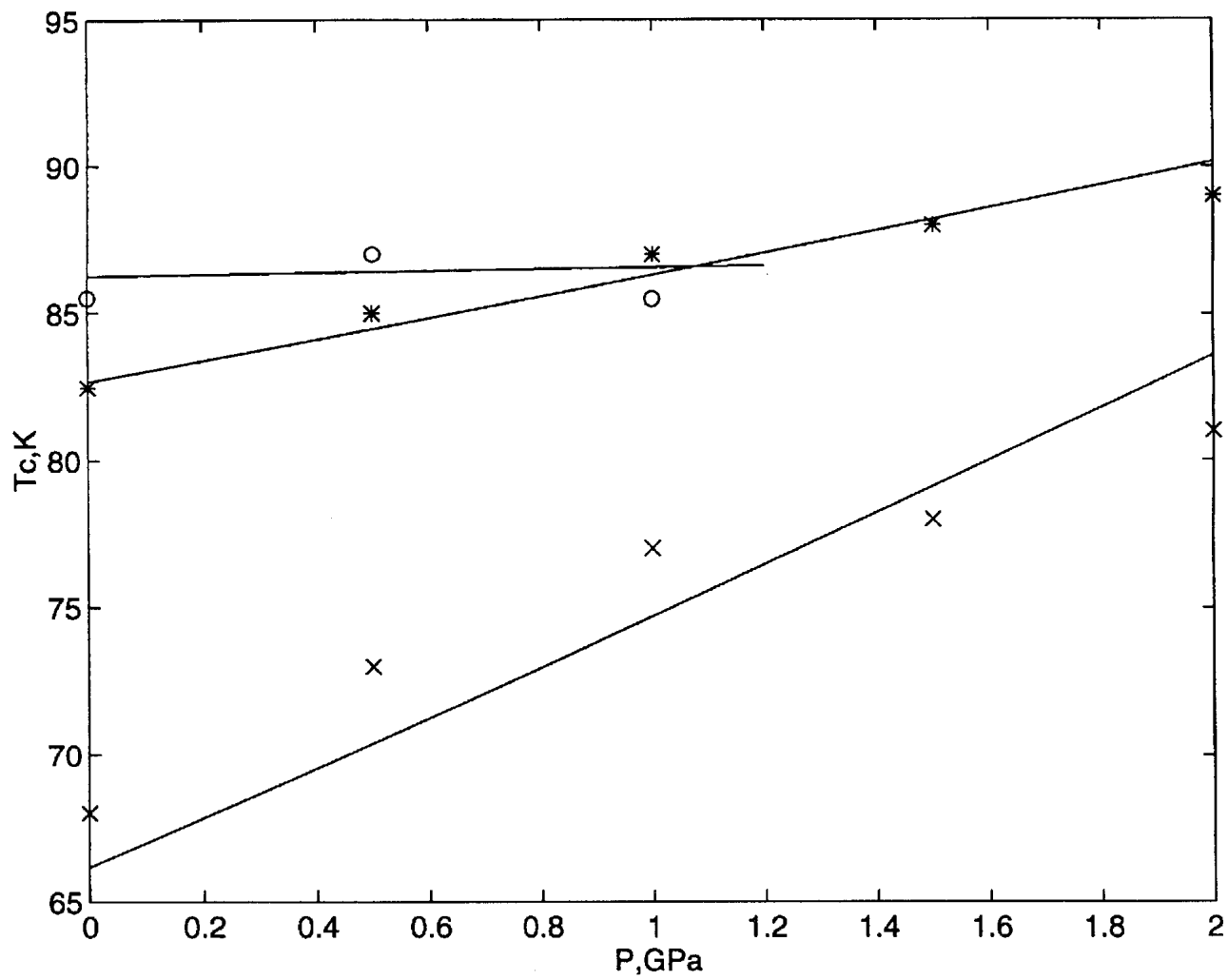


Figure 6